



Journal of the European Ceramic Society 31 (2011) 1199–1210

www.elsevier.com/locate/jeurceramsoc

# Crack propagation and stress distribution in binary and ternary directionally solidified eutectic ceramics

L. Perrière <sup>a,b</sup>, R. Valle <sup>a,\*</sup>, N. Carrère <sup>a</sup>, G. Gouadec <sup>c</sup>, Ph. Colomban <sup>c</sup>, S. Lartigue-Korinek <sup>b</sup>, L. Mazerolles <sup>b</sup>, M. Parlier <sup>a</sup>

<sup>a</sup> ONERA/DMSC, 29 avenue de la Division Leclerc, F-92322 Châtillon, France <sup>b</sup> ICMPE, UMR 7182, CNRS-Univ. Paris Est, 2-8 rue H. Dunant, F-94320 Thiais, France <sup>c</sup> LADIR, UMR 7075, CNRS-Univ. P. et M. Curie (Paris 6), 2-8 rue H. Dunant, F-94320 Thiais, France

#### **Abstract**

The development of directionally solidified eutectic (DSE) ceramics for gas turbine applications necessitates improving their strength and toughness. The early stage of crack propagation is investigated in either binary ( $Al_2O_3/Y_3Al_5O_{12}$ ,  $Al_2O_3/GdAlO_3$  and  $Al_2O_3/Er_3Al_5O_{12}$ ) or ternary ( $Al_2O_3/Y_3Al_5O_{12}/ZrO_2$ ,  $Al_2O_3/GdAlO_3/ZrO_2$  and  $Al_2O_3/Er_3Al_5O_{12}/ZrO_2$ ) DSE ceramics. *Post-mortem* scanning electron microscopy (SEM) examination of biaxial flexure induced cracks revealed crack deflection and branching in the various phases and in the phase boundaries. These observations are correlated to analytical and finite element (FE) internal stress calculations, FE determination of the axial shear stress component in the interfaces in the vicinity of the specimen surface (free-edge effect) and FE calculations of the stress distribution resulting from an applied loading. Results from ruby ( $Cr^{3+}$ ) fluorescence piezo-spectroscopy measurements are analyzed, taking into account the hydrostatic and plane stress hypotheses. Moreover, transmission electron microscopy (TEM) examinations have confirmed the role of interfaces in the crack nucleation and propagation modes.

© 2010 Elsevier Ltd. All rights reserved.

Keywords: Eutectic ceramics: Composites; Al<sub>2</sub>O<sub>3</sub>; Fracture; Residual stresses

### 1. Introduction

The development of new ultra high temperature structural materials in the aerospace field and in particular for gas turbine applications is a real challenge. Despite the various studies performed to increase the heat-resistance of nickel-based superalloys, their use at temperatures beyond 1400 K remains difficult. For higher temperatures, sintered ceramic oxides offer many advantages compared to superalloys: resistance to oxidation and abrasion, lower density. Unfortunately, sintered ceramics are brittle and their failure strength decreases when the temperature increases. Ceramic materials prepared from oxides by unidirectional solidification from the melt (melt growth composites (MGC)) add new potentialities to the advantages of sintered ceramics: a higher strength, almost constant up to temperatures close to the melting point (no amorphous phases at the inter-

faces), good creep resistance, stability of the microstructure and no chemical reaction between the constituent phases. 1-3 The microstructure of directionally solidified eutectic (DSE) ceramics consists in three-dimensional (3-D) and continuous interconnected networks of single-crystal eutectic phases. After solidification of binary eutectics, the eutectic phases are alumina and either an LnAlO<sub>3</sub> perovskite phase (Ln, lanthanide element: Gd, Eu) or an Ln<sub>3</sub>Al<sub>5</sub>O<sub>12</sub> garnet phase (Ln: Y, Yb, Er, Dy). In the case of ternary systems, zirconia is added as a third phase in order to refine the microstructure and to promote energy dispersive crack deflection modes acting in favour of a better toughness. In the present case, the directionally solidified eutectic ceramics under investigation are either binary (Al<sub>2</sub>O<sub>3</sub>/Y<sub>3</sub>Al<sub>5</sub>O<sub>12</sub> (YAG), Al<sub>2</sub>O<sub>3</sub>/Er<sub>3</sub>Al<sub>5</sub>O<sub>12</sub> (EAG) and Al<sub>2</sub>O<sub>3</sub>/GdAlO<sub>3</sub> (GAP)) or ternary (Al<sub>2</sub>O<sub>3</sub>/YAG/ZrO<sub>2</sub>, Al<sub>2</sub>O<sub>3</sub>/EAG/ZrO<sub>2</sub> and Al<sub>2</sub>O<sub>3</sub>/GAP/ZrO<sub>2</sub>) eutectics. Studies to control the microstructure of directionally solidified eutectic ceramics have been performed, acting on the processing parameters of the floating-zone method (arc image furnace).<sup>4-8</sup> The mechanical properties have thus been investigated on the small specimens manufactured through this

<sup>\*</sup> Corresponding author. Tel.: +33 1 46 73 45 69; fax: +33 1 46 73 41 42. *E-mail address:* roger.valle@onera.fr (R. Valle).

process. A biaxial testing disc flexure device has been used to investigate the early stage of crack propagation in the interconnected microstructure of the DSE ceramics. Post-mortem scanning electron microscopy (SEM) examination of the biaxial flexure induced cracks is focused on the possibility of crack deflection in the various phases and in the phase boundaries, a phenomenon which may markedly improve the toughness of these eutectic composites. However, the mechanical properties and the crack propagation modes depend on the level of the internal thermal stresses. In this context, internal stresses measurements have already been performed in eutectic ceramics using either X-ray<sup>10,11</sup> or neutron<sup>12</sup> diffraction techniques or fluorescence piezo-spectroscopy. 3,13–15 Analytical and finite element (FE) calculations of the thermal mismatch stresses can also be performed; they however require the prior knowledge of the thermomechanical parameters of the various phases 16-24 and of the eutectic composites.<sup>25</sup>

Consequently, complementary measurements have been performed, not only on the eutectic composites, but also on the individual garnet and perovskite phases. Even if analytical calculations had already provided a good estimate of the residual stress level in the vicinity of the interfaces in the simple configuration of infinite concentric cylinders, <sup>9</sup> additional FE stress calculations have been performed in order to map the stress components in more complex geometrical configurations. Moreover, concerning the free-edge effect in the vicinity of the specimen surface, FE calculations have permitted to determine the axial shear stress component in the interfaces. Internal stress measurements through ruby (Cr<sup>3+</sup>) fluorescence piezo-spectroscopy have provided an average value of the stress state in the alumina phase of the various investigated DSE composites. The fluorescence signal being emitted from a small depth interaction volume, FE calculations, taking into account the presence of the neighbouring surface, have allowed comparing these experimental results with those of analytical and FE calculations representative of the bulk material. Furthermore, transmission electron microscopy (TEM) examinations were performed in order to investigate, at a finer scale, the role of the interfaces in crack nucleation and propagation. Finally, a comparative analysis of all these complementary experimental and calculated results was aimed at a better understanding of the role of the interfaces in the fracture modes and on the toughness of the DSE composites.

## 2. Experimental procedures

# 2.1. Materials

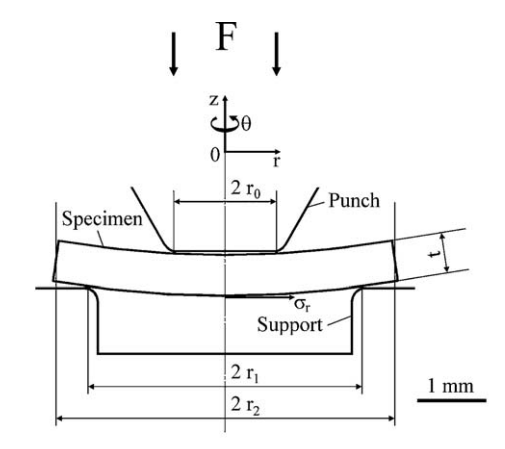
Eutectic samples are prepared from high purity powders (Al<sub>2</sub>O<sub>3</sub>: Baikowski Chimie, France; Y<sub>2</sub>O<sub>3</sub>, Er<sub>2</sub>O<sub>3</sub>, Gd<sub>2</sub>O<sub>3</sub>: Rhodia, formerly Rhône Poulenc, France; ZrO<sub>2</sub>: Th. Gold-schmidt Industriechemikalien, Germany) mixed at the ratios corresponding to the eutectic compositions.<sup>4,26–30</sup> Rods, isostatically pressed at room temperature, are then sintered at 1675 K for 10 h in order to improve their handling strength. Directional solidification is performed in air using the floating-zone trans-

lation technique (6 kW xenon lamp arc image furnace) at a solidification rate of  $10 \, \text{mm h}^{-1}$ , or  $20 \, \text{mm h}^{-1}$  in the only case of Al<sub>2</sub>O<sub>3</sub>/EAG/ZrO<sub>2</sub>. Final rods of oriented eutectics are about 6–8 mm in diameter and 40–60 mm in length.

#### 2.2. Biaxial flexure testing

Biaxial flexure testing was preferred to beam-bending tests since the coaxial-ring test is free of edge condition influences<sup>31</sup>: cracks initiate in the central area and propagate outwardly. On the contrary, the beam-bending test is influenced markedly by the edges parallel to the specimen major axis, the presence of flaws leading to premature and non-representative crack initiation. The biaxial disc flexure testing device<sup>9</sup> presents the ring supported/ring loaded test geometry (Fig. 1). The stress components may thus be determined through an analytical calculation.<sup>32</sup> In the central area (Fig. 1), inside the inner loading ring  $(0 \le r \le r_0)$ , the radial  $(\sigma_r)$  and tangential  $(\sigma_{\theta})$  stress components are equal, uniform and maximum. The main advantage of this system, as concerns the initiation of cracks and the early stage of crack propagation, is thus the possibility to subject the relatively large central area, which is free from edge defects, to a uniform biaxial tensile loading.

Specimens for the biaxial bending tests ( $\approx 800~\mu m$  in thickness) are cut perpendicularly to the growth axis of the 8 mm in diameter eutectic rods, the 5 mm in diameter discs being then cut in the central area of the slice. High quality surface finish of the lower surface of the specimen (i.e. the surface which will be subjected to the biaxial tensile loading), is obtained through diamond polishing. The biaxial bending tests are conducted at room temperature. After the flexure tests, examination of cracks is performed through scanning electron microscopy (SEM): Zeiss Gemini (field emission gun (FEG)-SEM).



$$\sigma_{_{T}}(r \leq r_{_{0}}, \theta) = \sigma_{_{\theta}}(r \leq r_{_{0}}, \theta) = \frac{3(1+\nu)F}{4\pi t^{2}} \left[ 2 \ln \frac{r_{_{1}}}{r_{_{0}}} + \frac{1-\nu}{1+\nu} \frac{r_{_{1}}^{2} - r_{_{0}}^{2}}{r_{_{1}}^{2}} \frac{r_{_{1}}^{2}}{r_{_{2}}^{2}} \right]$$

Fig. 1. Biaxial disc flexure test: the specimen under biaxial loading between the flat-ended punch (radius  $r_0$ ) and the support (radius  $r_1$ ), with specimen overhang  $(r_2-r_1)$ . In the central area, the radial  $(\sigma_r)$  and tangential  $(\sigma_\theta)$  stress components are equal, uniform and maximum  $(F: \text{applied force}, \nu: \text{Poisson's ratio of the specimen}, t: \text{specimen thickness}).$ 

# Download English Version:

# https://daneshyari.com/en/article/1476309

Download Persian Version:

https://daneshyari.com/article/1476309

<u>Daneshyari.com</u>